

Gentle Giant: A Power-Factor-Corrected Musical Tesla Coil

By
Ali Mouayad Albaghdadi
Kartik Singh Maisnam

Final Report for ECE 445, Senior Design, Spring 2025

TA: Liu Shengyan

6 May 2025

Team 68

Abstract

Our team envisioned and designed a dual-resonant solid state Tesla coil (DRSSTC) with active power factor correction that could be used to play musical notes. The DRSSTC operates off of AC mains wall power and produces large arcs from the top. Musical notes and power level/arc length can be changed through an optically coupled remote signal called an interrupter.

The design was motivated by a desire to advance the Tesla coil frontier, which has not changed since the designs of Steve Ward and Gao Guangyan over a decade ago. Our theoretical analysis determined such a design would be feasible. However, due to critical component shortages and failures, the project was not demonstrable within the time limit.

Table of Contents -

1. Introduction
2. Design
 - 2.1. Design Procedure
 - 2.2. Design Details
3. Verification
4. Cost
 - 4.1. Parts
 - 4.2. Labor
5. Conclusion
 - 5.1. Accomplishments
 - 5.2. Uncertainties
 - 5.3. Ethical Considerations
 - 5.4. Future Work
6. References

1. Introduction

Tesla coils are impressive visual and auditory devices; some can create a surprising range of sounds using arc discharges, and thus have found uses as display pieces in entertainment and STEM education. A particularly large one is permanently mounted to a ceiling inside the Museum of Science and Industry in Chicago. However, for the majority of their existence, they have been crude instruments. Their design and operation typically results in a suboptimal use of AC power, also known as a poor power factor, and even with the advent of "solid-state" Tesla coils (SSTCs) that use power semiconductors, the situation has not improved. Areas with lower-voltage mains like the United States are often at a disadvantage due to details in many of these implementations.

Further, when scaling up to large Tesla coils for use in performances, they can place significant strain on electrical grids and suppliers. Addressing these challenges could enhance the efficiency and portability of all Tesla coils, making them more practical for a wider range of applications.

In response to these issues, we designed and built a Dual-Resonance Solid State Tesla Coil (DRSSTC) with an active Power Factor Correction (PFC) front end. The combination of these two systems, the latter of which has never been done before on a Tesla coil, puts our design at the very forefront of Tesla coil power electronics technology, and would solve several technical issues with other modern designs.

Tesla coils are effectively giant transformers, with a secondary winding that has many times more turns than the primary. Conventional SSTCs operate by first rectifying mains AC to a high-voltage DC, then using a half-bridge or full-bridge of power semiconductors to switch the primary of the Tesla coil. This results in a very large voltage being generated in the secondary, which causes it to release arc discharges. A major benefit that DRSSTCs like ours have over SSTCs is that it operates more like a resonant converter. In the design phase of the transformer, the primary and secondary must be tuned to have close LC resonant frequencies. During operation, feedback from the primary is used to switch it at its resonant frequency, which results in more energy being built up in the system and more impressive arc discharges. This energy buildup must be stopped intermittently by an external PWM signal called an interrupter (which can simultaneously be used to modulate musical sounds into the arc discharges). The primary feedback also enables zero-current switching (ZCS), reducing thermal losses in the power stage to near zero.

We choose to improve even further by designing a digitally controlled boost-type active PFC to create the high-voltage DC rail. This brings with it several benefits of its own, like improving system power factor and making the system agnostic to mains voltage and frequency. With a higher power factor, larger arcs can be generated for the same apparent power, or arcs of the

same size can be generated for less apparent power. This is a great all-around benefit for Tesla coil efficiency and viability at large scale.

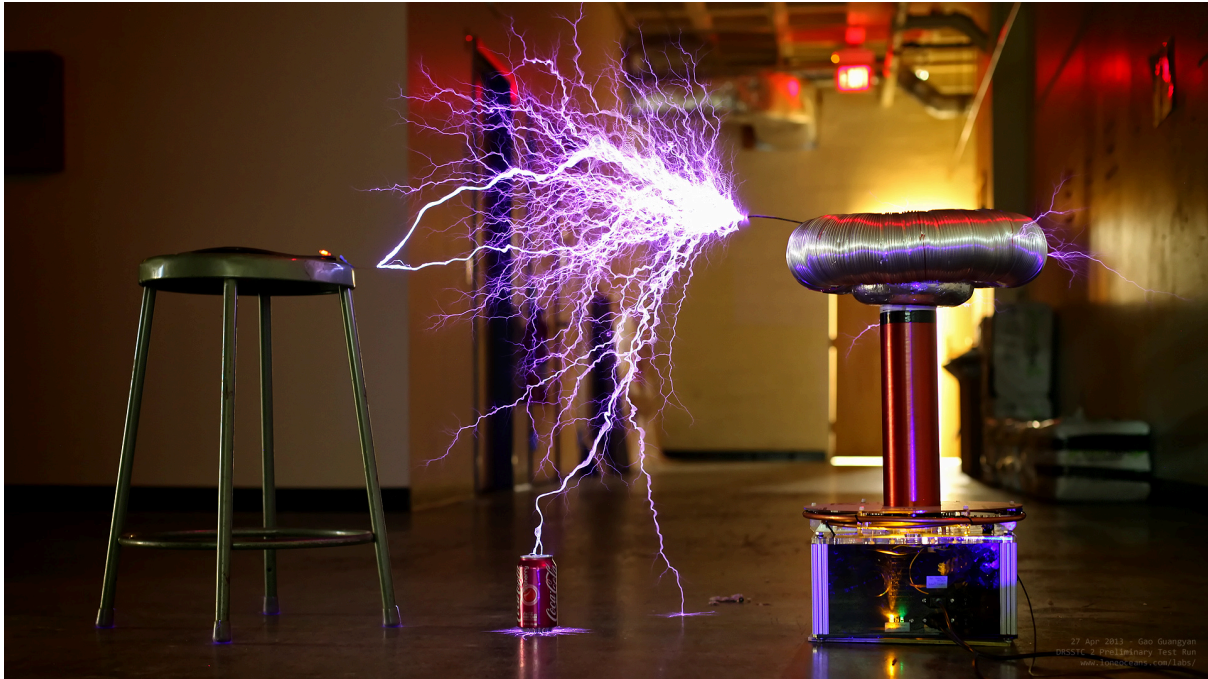


Figure 1. One of the first dual-resonant solid-state Tesla coils in operation. Photo courtesy of Gao Guangyan.

As our main focus will be the design and operation of the active PFC, users will not immediately see any visual differences from other Tesla coils. However, a measurable metric can be provided in the form of the device's power factor and power consumption.

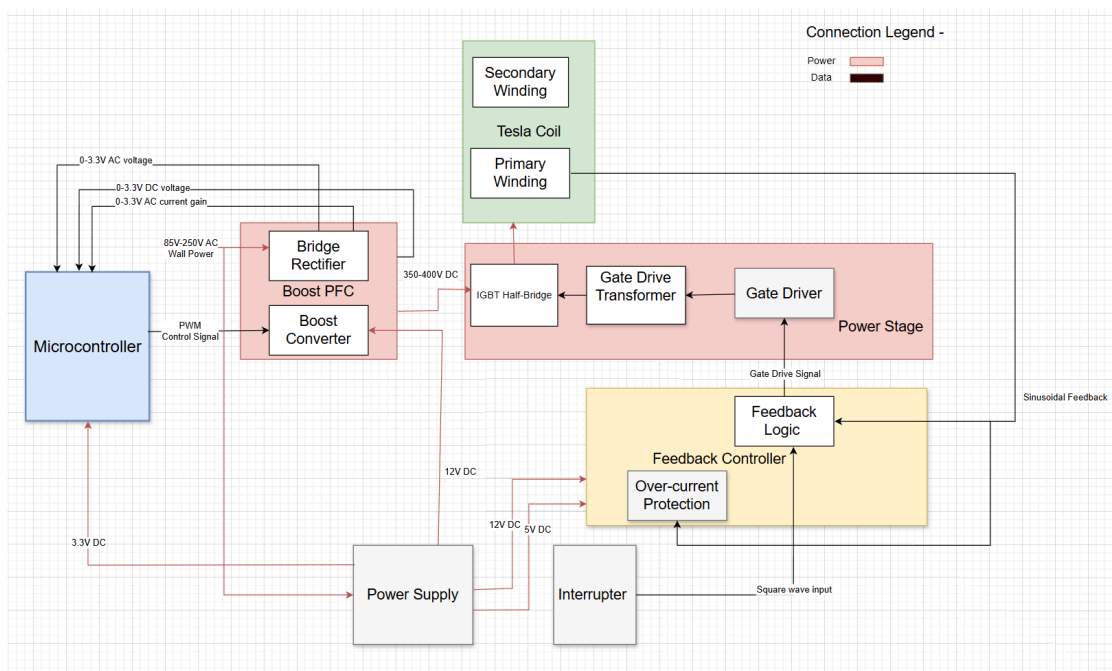


Figure 2. Overall block diagram of our design.

2. Design

2.1. Design Procedure

2.1.1. Tesla coil subsystem

We considered the physical construction of the Tesla coil to be its own subsystem despite its lack of electronic components in and of itself. As previously mentioned, a Tesla coil is effectively a large air-core transformer, meaning it consists of a primary and a secondary. To generate a high voltage, the secondary must first be wound with many more turns than the primary, and then the primary winding must be oscillated. This causes current to flow in the primary, inducing a directed EMF that then induces a much larger voltage in the secondary. Solid-state Tesla coils (SSTCs) utilize solid-state electronics (like FETs or IGBTs) to forcibly oscillate the primary by switching a DC voltage across it. The latest innovation, dual-resonant solid-state tesla coils, use a film capacitor in series with the primary inductor to cancel out the reactance and allow for current to build up more easily. During the design, they must also carefully ensure that the primary and secondary LC resonant frequencies are close. These two steps together allow them to utilize primary feedback: the primary is driven at its own resonant frequency (rather than that of the secondary), which subsequently causes resonance in the secondary, leading to much better energy buildup and transfer. We estimated from anecdotal reports of DRSSTCs of similar size that Gentle Giant would reach maximum current amplitudes of around 300A in the primary.

The physical design of a Tesla coil, as well as the calculation of the LC resonant frequency of the secondary, is a slightly unrigorous process. The “topload,” the toroidal or spherical metal structure on top of all DRSSTCs and most Tesla coils in general, acts as a capacitor to ground. It is a highly variable capacitance, and not much simulation work has been done in the field to determine how the charge field behaves under high voltages, different atmospheric conditions and arc discharges. Thankfully, a “good enough” approximation tool exists in the form of JavaTC, an online calculator for Tesla coil design. Once the physical parameters of the coil are added to the calculator, it finds many useful parameters about the Tesla coil, including the resonant frequencies, the transformer coupling coefficient, and more. A screenshot of our JavaTC run for our design can be found in Appendix B, and the design will be discussed in further detail in section 2.2.

2.1.2. Power stage subsystem

The power stage is what actually drives the primary winding at its resonant frequency. It is a relatively simple subsystem: it consists of a half-bridge of IGBTs, their gate drive circuitry, and a pair of film capacitors to suspend the other end of the primary at half of +PWR. In this case, +PWR is 400VDC, and is generated by the boost PFC frontend detailed in 2.1.3. The primary connects via the J6 screw terminal and is subsequently oscillated between +PWR/2 and -PWR/2 by Q1 and Q2.

Q1 and Q2 were chosen to be the FGA60N65SMD IGBT, a high-current 650V IGBT with an isolated thermal package that is also common in other DRSSTC designs. R11 and R12 are gate drive limiting resistors, whereas D7 and D15 act as fast discharge paths to further ensure that an IGBT turns off before the other turns on (preventing shoot-through currents). D16 and D17 are bidirectional TVS diodes, protecting the gates of the IGBTs from any stray spikes from the Gate Drive Transformer (GDT).

The GDT is our chosen solution to drive the half-bridge. IGBTs, like MOSFETs, require a voltage difference between their gate pin and lower potential, but Q1's lower potential is unknown and potentially at +PWR/2 or higher. The GDT utilizes the fundamental fact that the output of a transformer is isolated from its input to change the ground potential of the drive signal to the emitter pin of Q1 (this is where GDT_A- goes). The drive signal is generated by the feedback controller, which is discussed in more detail in 2.1.4. We could have used an isolated gate drive IC and isolated supplies, but decided against it due to their complexity; GDTs are very common in Tesla coil drivers in general for their cost-effectiveness and simplicity.

GDTs for driving half-bridges are constructed by wrapping three wires around the same ferrite core. One is connected to a driver circuit (in this case, the DRIVER+/- pins of the feedback controller in 2.1.4) and the other two are connected to the IGBTs' gate and emitter pins. Here, they are connected to A+/A- and B+/B- respectively.

This is the extent of the power stage design; the design details in section 2.2.4 will follow how the power stage was laid out and thermally managed.

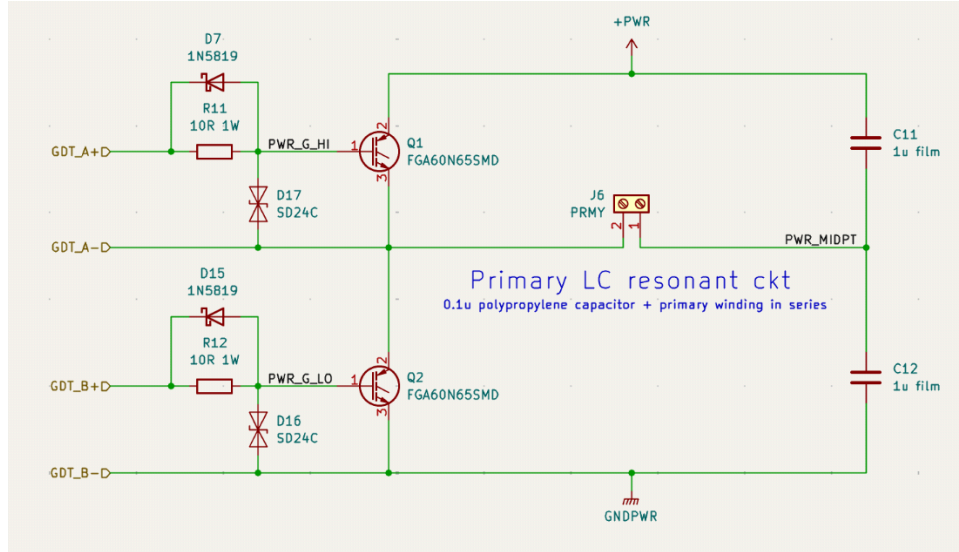


Figure 3. Schematic diagram of the power stage.

2.1.3. PFC subsystem

Passive power factor correction is typically done by adjusting the impedance of an AC circuit using inductors or capacitors, but this is not useful due to the way a solid-state Tesla coil operates. Arcs are discharged (and subsequently the load spikes) at almost random intervals due to the plasma physics of the surrounding air, so like with other switching power supplies in consumer electronics, we saw fit to use an active PFC frontend so it could compensate for rapidly changing load. Several types of active PFC topologies exist, including boost-type, AC-switch bridgeless, and totem-pole PFC. All perform the same task: take in an AC voltage and generate a DC voltage while maintaining both active control of the DC voltage and a perfect sinusoid of current draw on the AC side that is in phase with the voltage. Each topology has its own advantages, but the topology we chose for our PFC stage was the boost-type PFC converter. This is due to its extreme simplicity to design and control: it requires a single actively controlled switch, whereas all other designs require at least two and recommend four to maximize their efficiency benefits.

Early Tesla coil designs operated off a DC voltage rail of 170V or 340V depending on the region that they were operated in. This is because with a straight diode + capacitor rectification method, the voltage produced is equal to the maximum amplitudes of $120V_{rms}$ and $240V_{rms}$ respectively. As part of our design philosophy was to make the operation of the coil region-agnostic, we chose to design for an input voltage range of $85-265V_{rms}$, encompassing all regions and their valid grid drops or spikes. This is a common voltage range on region-agnostic consumer electronics as well. In a boost PFC, the output DC voltage must be at least as high as

the peak of the AC wave, which means we had to make ours at least $265V \times \sqrt{2} = 375V$. Thus, our PFC stage targeted an output voltage of 400VDC for use by the power stage.

Active PFCs need some sort of digital control device to frequently read the state of the system and adjust to keep both the input current sinusoidal and the output voltage regulated, as well as compensate for different mains voltages and frequencies. For our system, we chose to utilize a microcontroller (heretofore referred to as the MCU) and write the control code ourselves. Specifically, an STmicroelectronics STM32F103C8 was selected for this task due to its availability, high trustedness and reliability, and high-resolution 12-bit ADCs (analog-digital converters).

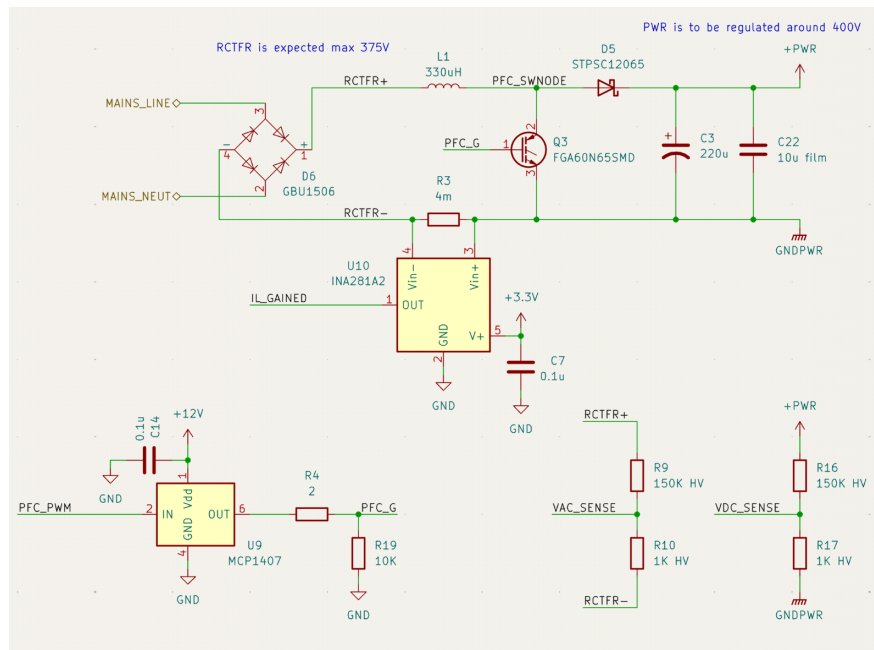


Figure 3. Schematic representation of the PFC subsystem.

The subsystem consists of a bridge rectifier and a boost converter structure, which can be further broken down into an input inductance, an output capacitance, an active switch and a diode. A gate driver powered from the 12V supply was used to allow the MCU to drive the IGBT, and a current sense amplifier and some voltage dividers allow the MCU to safely read the state of the system using its ADCs.

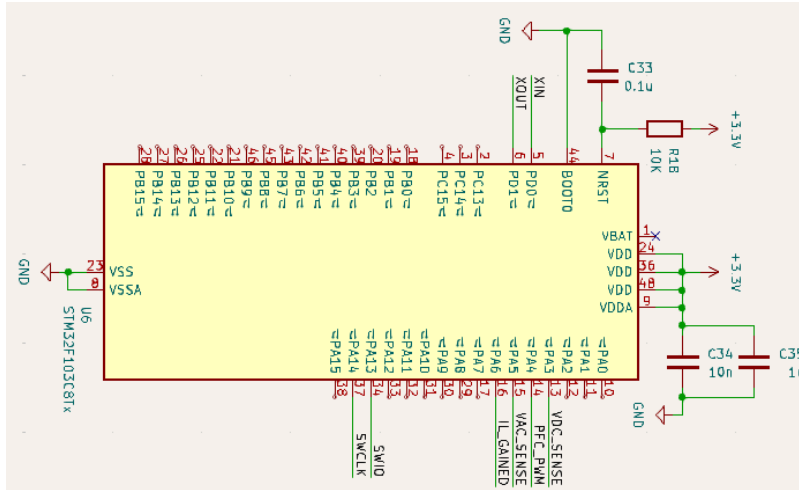


Figure 4. Schematic Representation of the STM32F103C8T6 microcontroller.

The MCU uses a high speed external oscillator (HSE) as a clock source and runs two timers: a trigger timer for ADC input measurement and a PWM output to the MOSFET, both with a frequency of 80kHz and variable duty cycles. This frequency was chosen in line with the recommendation in [6].

The input AC voltage, output DC voltage and input AC current are amplified or divided as needed and used as inputs to the ADC pins on the MCU, and these readings are stored into memory for direct access by the control routine.

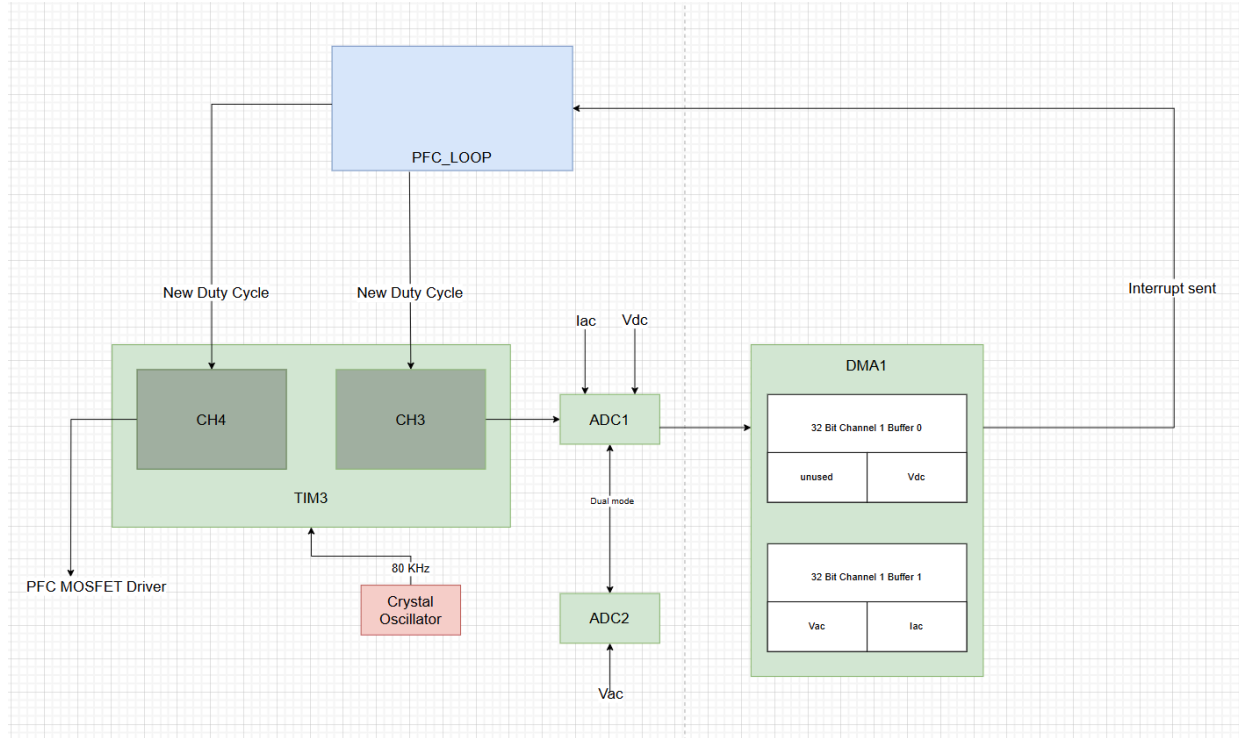


Figure 5. Block Diagram representation of the MCU's channel-to-channel pipeline.

The block diagram shown in figure 4 represents the overall pipeline and organization of the MCU's inputs, timers, and outputs. Once all three inputs have been read and stored in memory, the control routine is started and changes the duty cycle of both trigger and PWM output, controlled by the error in calculated demand current to the input current explored in detail ahead.

2.1.4. Feedback controller subsystem

The feedback controller subsystem is largely the work of Steve Ward [11], with minor adaptations to fit our part choice standards as well as replace obsolete components. We did not invent the core working principle of this subsystem, so we will not discuss it further in 2.2, instead focusing on the interrupter we built to interface with it. It serves a simple and fixed purpose in our larger design: it makes the DRSSTC work as a DRSSTC, our load of choice for our active PFC. It drives the primary winding of the Tesla coil at its resonant frequency using ZCS (Zero-Current Switching) while stopping the ring-up from getting too high using either an external interrupter signal or an overcurrent detector (whichever trips first). The former can, as previously mentioned, be used to modulate musical sounds into primary, which then carries over into the arc discharges out of the secondary.

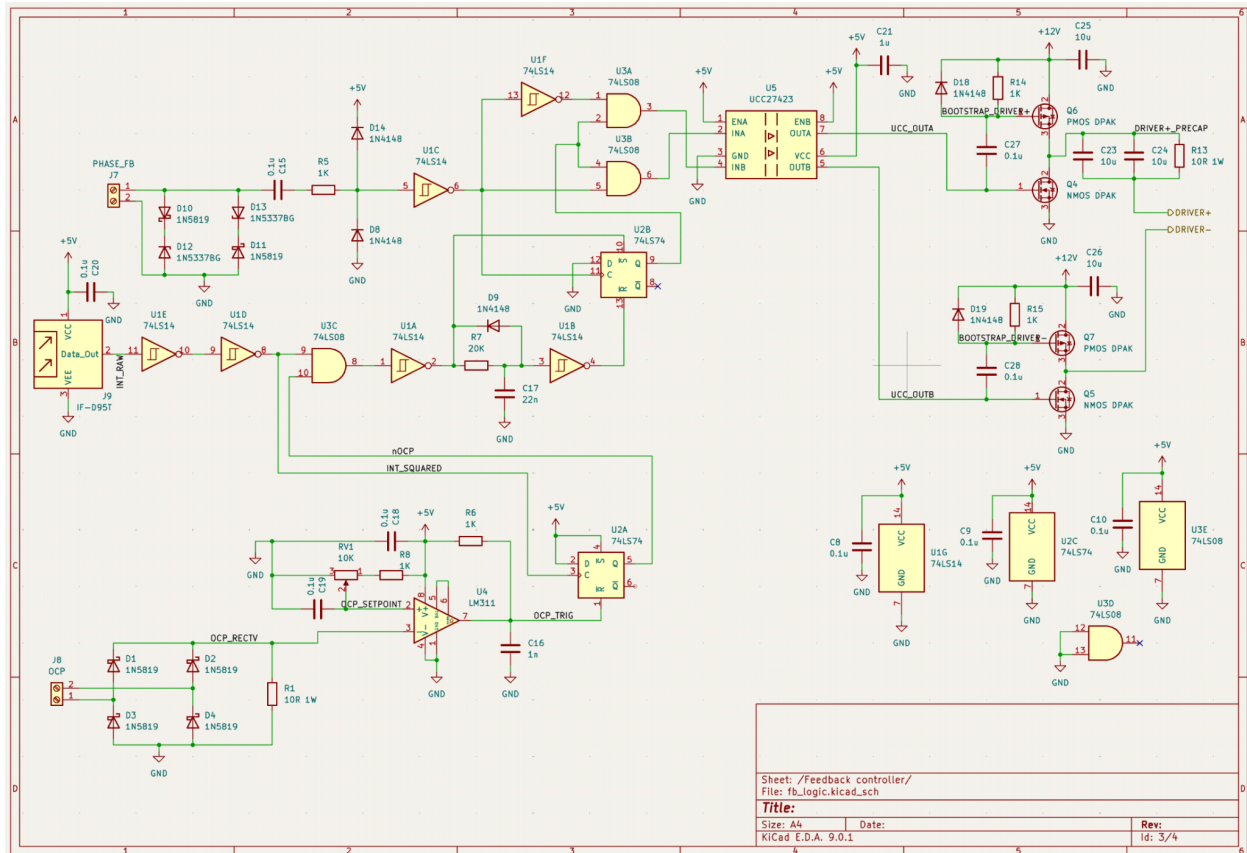


Figure 5. Schematic representation of the feedback controller subsystem.

The 74LS series of logic chips was used in conjunction with many diodes and an LM311 comparator to implement both a resonant feedback driver as well as two interruption sources. The inputs to the screw terminals PHASE_FB and OCP are current transformers: ferrite cores with a small wire wrapped around them through which the larger primary wire passes. The small wire is then connected at both ends to the screw terminals. When the primary oscillates, a similar current sinusoid is induced in the wires whose amplitude is that of the current in the primary divided by the number of small wire turns. At PHASE_FB, the current sinusoid is clipped and squared up to provide an accurate “digital” zero-crossing detection. At OCP, the sinusoid is full-wave rectified and put across a burden resistor, then compared to a known voltage using a comparator and a setpoint set by a potentiometer. This ensures that the amplitude of the current in the primary never goes above a chosen value. If the comparator’s output OCP_TRIG goes low, it causes the latch U2A to reset and send nOCP low. It can be set the next time the interrupter square wave, INT_SQUARED, goes high, as D is tied high. Ultimately, when the OCP trips or the interrupter goes low, it stops the FB signal from doing anything, as pins 2 and 4 of the AND gate chip U3 go low. Those AND gates switch two P-N MOSFET pairs (through a gate driver U5) which drive the Gate Drive Transformer (GDT) discussed in section 2.1.2. The GDT

drives the gates of the power stage IGBTs, and thus the feedback system drives the power stage with ZCS.

More advanced controllers, such as the one designed by Gao Guangyan [3], implement something called phase lead, which utilizes an adjustable inductor, a gyrator circuit, or any adjacent solution to lead the phase of the FB signal slightly. This is because the power stage can only switch after the feedback controller detects a zero crossing, it propagates through the logic, through the P-N pairs, across the gate drive transformer, and finally after the switching delay of the power stage IGBTs. Phase lead results in better zero-current switching, but we left it out for simplicity reasons. It could be added to a later version without issue.

2.2. Design Details

2.2.1. Tesla coil subsystem

We wanted to build a Tesla coil that wasn't too large so that it could be built and moved around quickly, so we designed the secondary winding to be 10 inches tall. (Note that in the picture in Appendix B, the secondary coil "starts" at 5 inches and "ends" at 15 inches. This is to allow for 5 inches of space underneath the coil for an electronics enclosure; 0 inches represents the ground for the calculation of stray capacitances like that of the topload.) The diameter was chosen for the use of a 2" inner-diameter PVC pipe as a winding form, which was freely available to us from an external source. We chose to wind 36 AWG enameled wire around it, as research on forums like the High Voltage Forum showed that it was a common wire gauge used by other TCs of similar scale. A sub-calculator informed us that it would take around 1700 turns of the enameled wire to make a winding 10 inches tall. The topload was then chosen to be a toroid and sized mostly for aesthetic purposes, as there are no hard requirements on its specifications if it is designed before the primary. This all resulted in a secondary F_{res} of 271.34kHz.

We then sized the primary inductance and capacitance to provide a close-but-not-exact match in resonant frequency, as well as an adequately low transformer coupling coefficient. A coupling coefficient that is too high would cause a dangerously fast ringup in the secondary winding, so a value < 0.2 is recommended. Through forum research, as well as studying Gao Guangyan's designs [3], we found that the Cornell Dubilier 940C and successor 942C were the most popular primary capacitors for small-scale Tesla coils. Most also used values in the 0.1uF range, so we chose a 0.1uF 942C and moved on to the primary inductance. We used 14-gauge wire, as it was a commonly used value in TCs of similar scale. We wanted a design where the primary windings were stacked vertically around the secondary, so we adjusted the number of turns and the spacing from the secondary until we reached adequate values: a primary F_{res} of 229.43kHz (detuned by 15.45% from the secondary) and a coupling coefficient of 0.194.

The primary winding that achieved these values was 0.6 inches tall and had a diameter of 3.5 inches, so we could move on to 3D modeling. We used FreeCAD to build a properly sized form for the primary to be wound on, as well as a toroid half that we could make two of and glue together. We 3D printed these, as well as some accessory hardware like end caps for the PVC pipes and a stand to make winding the secondary easier, on a Bambu Lab P1S FDM 3D printer using PLA filament.

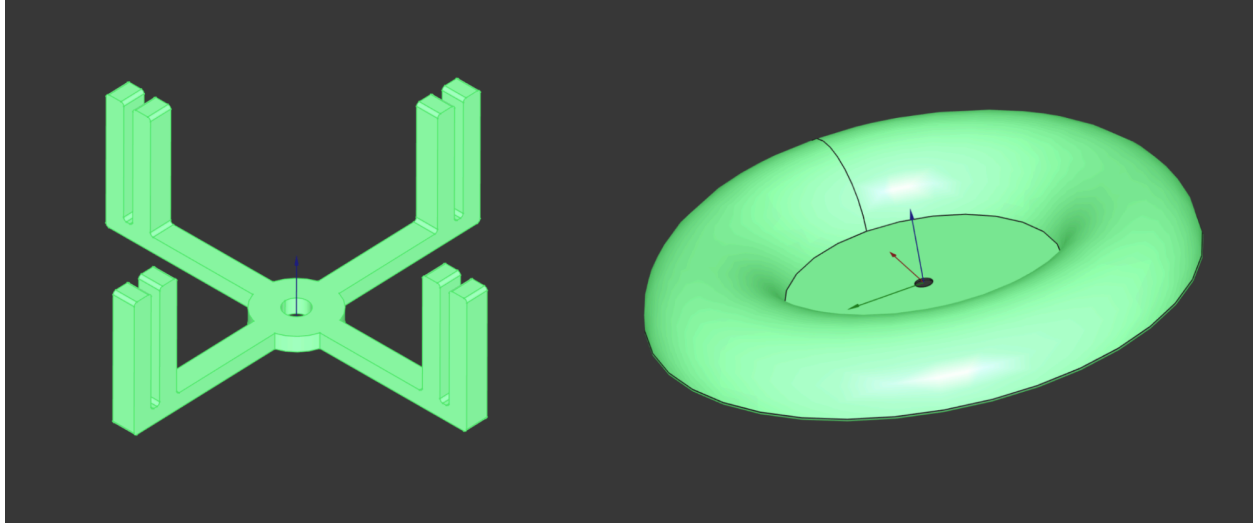


Figure 6. FreeCAD renderings of the primary form and toroid half (not to scale).

With this, we were satisfied with the design as an initial step and could proceed, knowing that we could later adjust the number of the primary windings as necessary to fine-tune its resonant frequency.

2.2.2. PFC subsystem

2.2.2.1. PFC power electronics

To design the PFC, we used the formulas in [5] as a guide for the majority of our design. All formulas explicitly written in this subsection are heretofore from [5]. We had two main requirements as given by our R&Vs: the PFC had to operate between 85 and 265V_{rms}, as well as consume no more than 1000VA. This meant a maximum power of 1000W if and when the power factor is unity. The output voltage has been previously determined to be 400VDC. The first formula was to determine the minimum required inductance:

$$L = \frac{1}{\%Ripple} \times \frac{V_{ac,min}^2}{P_o} \left(\frac{1 - \sqrt{2} \times V_{ac,min}}{P_o} \right) \times T, \text{ where } T \text{ is the reciprocal of the previously chosen}$$

switching frequency. With a ripple percentage chosen to be 30% as recommended, this gave us a minimum L of 210.57uH, which we then scaled up to 330uH for margin of safety. We then wanted to ensure that any core we picked would not saturate, so we used the formula

$$I_{L,max} = \frac{\sqrt{2} \times P_o}{V_{ac,min}} \times \left(1 + \frac{\%Ripple}{2}\right)$$

to calculate that the maximum inductor current would be around 19 A. Using the skin effect formula and calculating the copper temperature rise, we determined that 17 AWG wire would be sufficient to carry this current under the worst possible case. We then identified the Kool Mu 0077439A7 ferrite core as a potential candidate for the PFC inductor core, and calculated the maximum H-field it would endure using the formula

$$H = \frac{0.4\pi \times N \times I_{L,max}}{l_e}, \text{ where } l_e \text{ is the effective length of the core in centimetres. } H \text{ was}$$

determined to be 12.45 kA/m, which did not saturate the core.

[5] states that the PFC diode should be rated for 1A continuous current for every 75W the PFC stage outputs. Since ours was to be rated for 1000W, we chose a 12A SiC Schottky diode. SiC Schottky chemistry was explicitly recommended due to its superior properties. We also chose the active switch to be the same 60N65 IGBT purely for simplicity reasons; the 60N65 datasheet also states its suitability for PFC applications. The output capacitance was also shared with the Tesla coil, so we chose a value of 220u electrolytic in parallel with a 10u film capacitor to match DRSTCs of similar size.

2.2.2.2. PFC control software

The MCU's code is given in Appendix C for further reference. This section will explain important initializations and the overall control process.

With the APB clock set to 8MHz, we used a counter period of 100 to get our required 80kHz frequency for Timer 3.

The scaling factor (x.1) gives us the conversion from analog to digital values and is a crucial part of converting the obtained values back into analog terms for convenient measurement through the conversion factor K, where R_{A1} and R_{A2} are the voltage divider resistors for the input voltage divider.

$$K = \frac{\frac{(2^{ADC \text{ bits}} - 1)}{ADC \text{ Range}}}{\frac{R_{A1} + R_{A2}}{Scaling \text{ Factor}}}$$

The trigger timer's duty cycle is kept to half the PWM's duty cycle to produce a smooth triangle signal as seen in Figure 7. At the first falling edge of the trigger in a new cycle, V_{dc} is measured and stored in buffer 0. During this process we set a "currentbuffer" variable to 1, marking the completion of the first

measurement. In the next falling edge of the trigger, I_{ac} and V_{ac} are measured, stored in buffer 1 and currentbuffer is set to 0. Now that we have all three input values stored, we call an interrupt to begin our control routine which then changes the duty cycle of both the PWM and trigger.

Digital PFC timing

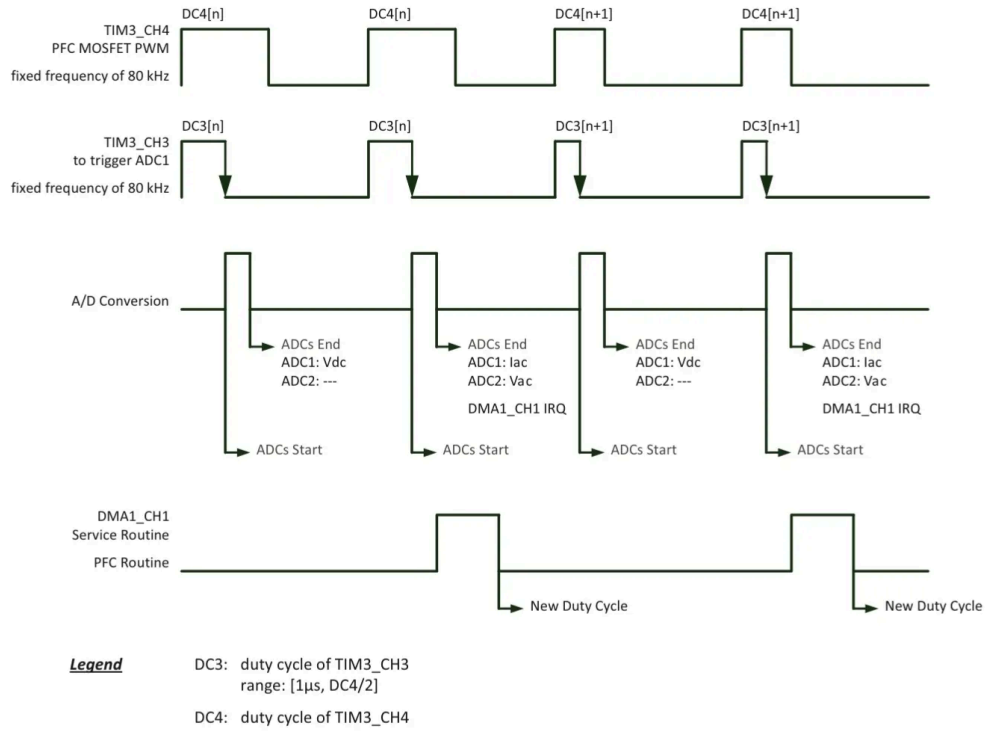


Figure 7. Timing diagram of the control routine.

In the control routine, we first convert the read ADC values to convenient 350-400V values using the voltage conversion factor given above. The demand current for the digital PFC [12] is calculated as follows -

$$I_{demand} = \frac{V_{ac} * V_{dc}}{(V_{rms})^2}$$

Where V_{rms} is roughly approximated using the following equation -

$$V_{rms} = 0.707V_{ac}$$

This demand current is then compared against the input current, and the new duty cycle is determined through this following equation -

$$New\ Duty\ Cycle = |I_{demand} - I_{ac}| * KP_{PFC} + KI_{PFC} * \int |I_{demand} - I_{ac}| dt$$

Here, proportional-integral controller gains were used to ensure stability of our PWM output. The proportional gain determines how much the PWM will vary in response to a change in demand versus input current, and was chosen to be about 0.02. The integral gain accounts for persistent offsets from the demand current and was set at 0.0005.

2.2.3. Feedback Controller

2.2.3.1. Feedback circuit

This circuit is comprised of simple logic that accepts a sinusoidal signal from the tesla coil and an interrupter signal and acts as overcurrent protection for the PCB.

2.2.3.2. Interrupter Circuit

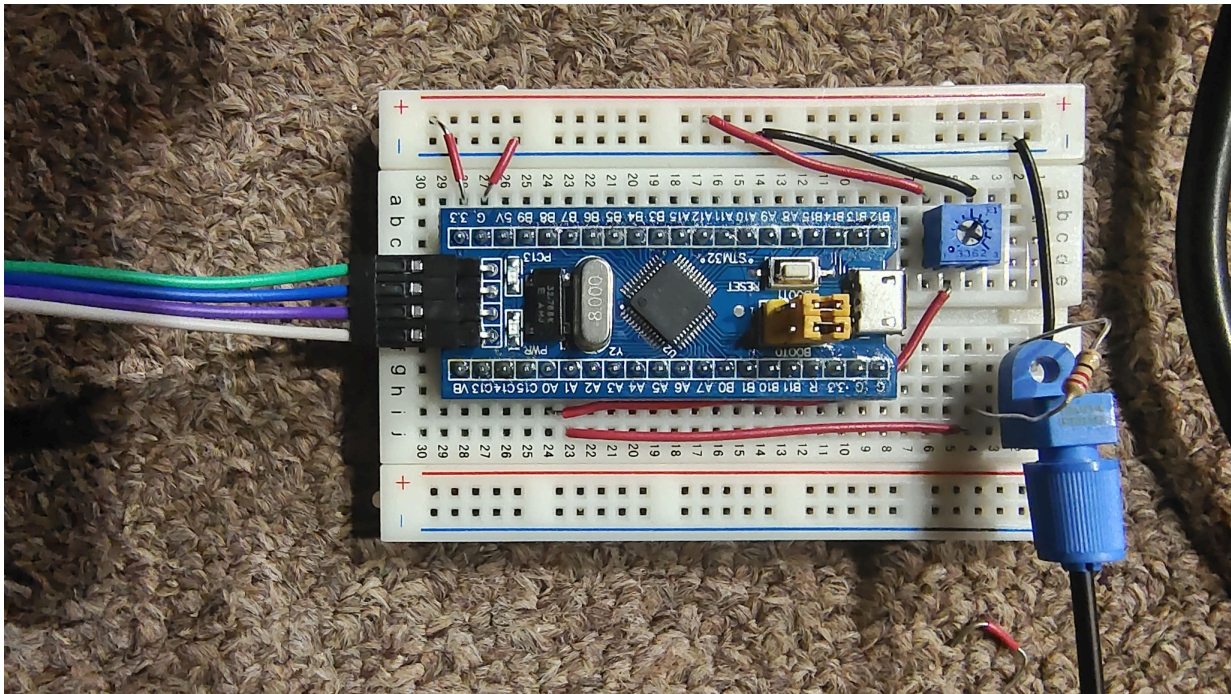


Figure 8. External interrupter circuit, connected to an IF-E91D optical transmitter.

We used an external interrupter circuit in order to control the coil's operation from a safe distance. This circuit uses an STM32F103C8T6 "Blue Pill" which outputs a square wave with a duty cycle of <20% adjustable using a 100kΩ potentiometer. This square wave goes through a 220Ω resistor and acts as an input to the IF-E91D optic transmitter. This signal is sent to the IF91D receiver through a long optic fiber cable as an input to the actual feedback controller.

2.2.4. PCB Design

The last step was to lay everything out on a PCB. One main rule prevailed: power loops should be as small as possible to minimize the EMI radiation and absorption. We eventually settled on the design shown below, and commissioned JLCPCB to manufacture it using a 2-layer board of 2oz/ft² copper. This double copper weight was necessary due to the main power flowing through the PCB. The mains AC input, 12V DC input, PFC inductor, primary winding, all three ends of the GDT, and the FB and OCP current transformers all connected via screw terminals placed around the perimeter and were labeled accordingly using silkscreen.

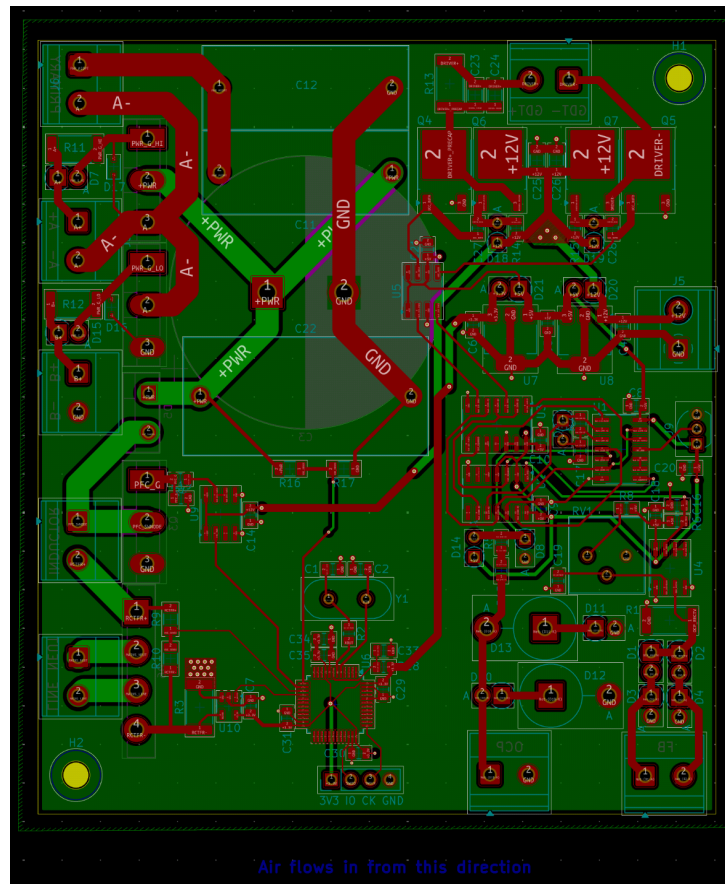


Figure 9. PCB layout of the completed Tesla coil system.

Capacitors were placed on both sides so that the whole design could be packed as efficiently as possible; the pads were positioned as close as possible to the capacitor on the opposite side. The thickest traces, carrying +PWR and the primary current, are 3mm wide. Combined with the 2oz copper weight, we used the IPC 2221 formula $I = K \times \Delta T^{0.44} \times (W \times H)^{0.725}$ as well as the copper fusing current formula to ensure that the traces would not be destroyed or have an

inordinate temperature rise in them during the 300A maximum current spike of the primary. The width chosen was determined to be sufficient.

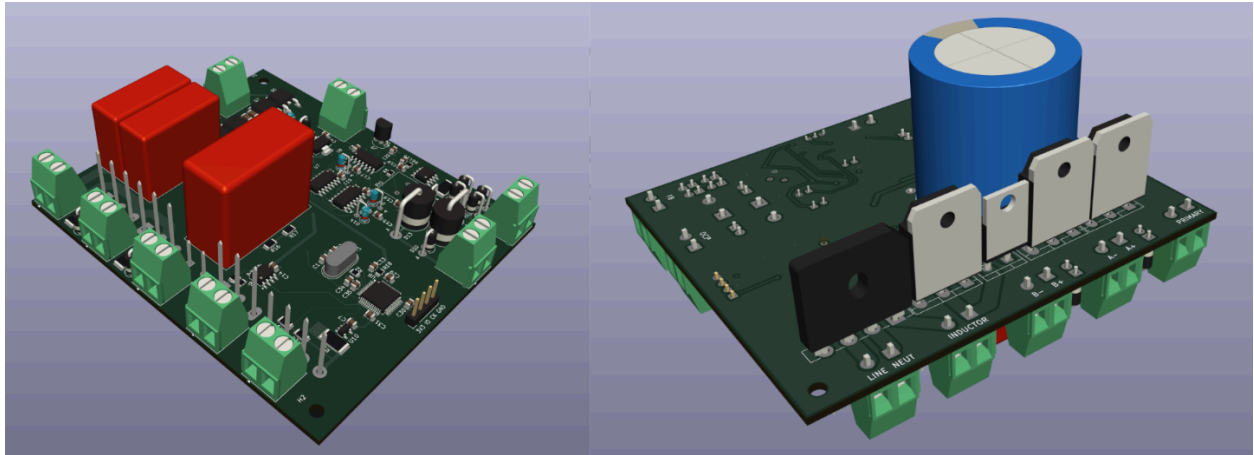


Figure 10. 3D models of the completed board.

The thermally constrained devices, namely the power stage IGBTs and the semiconductor devices in the PFC stage, were lined up on the reverse side of the board so they could be cooled with one heatsink going across. However, since heatsinks are made of metal, we did not want to have the entire heatsink sitting at a high DC voltage, nor did we want two devices to short to one another through the heatsink. The 60N65 IGBTs have an electrically isolated thermal interface surface, and the diode bridge was encased in plastic, but the SiC Schottky package was not isolated. We opted to use an electrically isolating thermal pad for it, and thermal grease for the rest of the components.

3. Verification

3.1. R&V Table

Our project level requirements were -

1. The measured power factor has to be above or equal to 0.95 when operating at the US mains level of 120VAC.
2. Arc discharge length has to be at least 1 foot, to demonstrate working of the Tesla coil.
3. The apparent power drawn during operation should be no more than 1000VA

However, we faced three critical part failures during the testing of our board, which limited our ability to test further in a meaningful manner. The following part failures were encountered -

IFD95T - optical transceiver damaged due to ESD, requiring a redesigned interrupter to send input to the Tesla coil. However, the alternative method found (running 5V square wave directly to the coil) was deemed to be too risky for the project.

Gate Driver MOSFET (Driver pair) - started smoking when the 12V power supply input was connected. A short was initially determined as the cause, but the localized failure of the component suggests it may have been damaged during the soldering process.

3.3V regulator - primary suspects are possible damage while soldering due to hot air gun or ESD damage from the environment. The remaining regulators were verified to be working using a multimeter..

3.2. Relevant Data

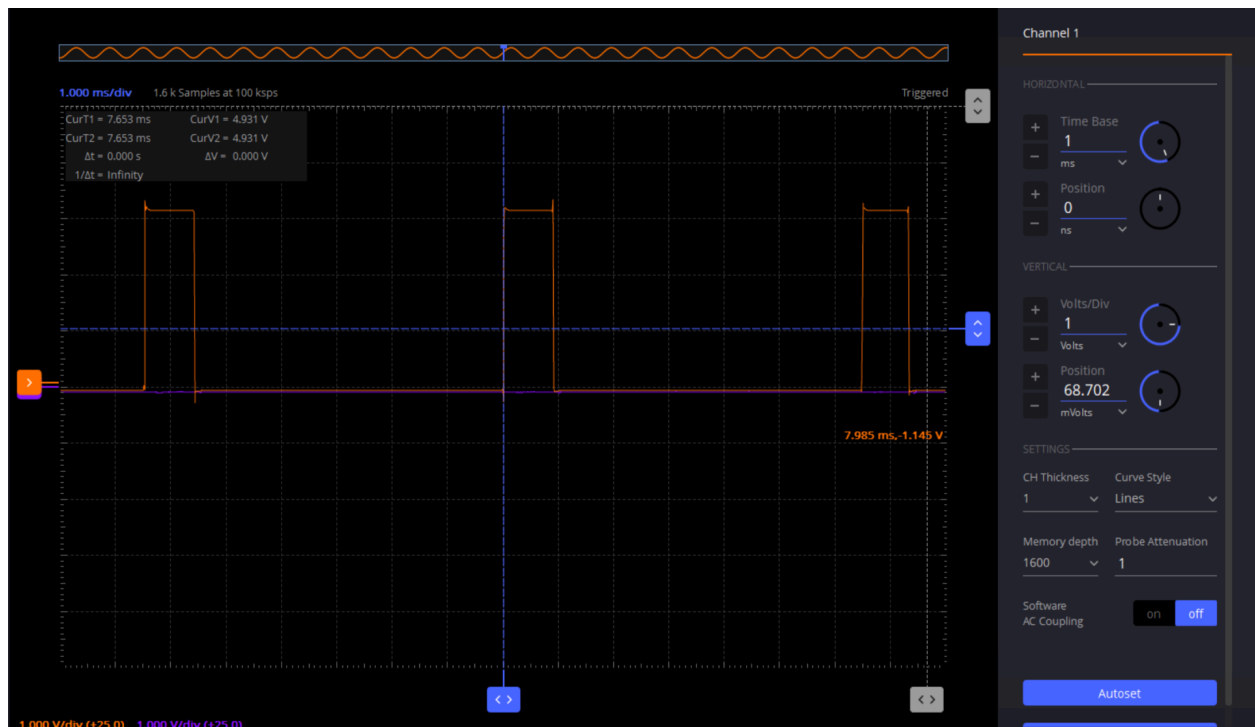


Figure . Interrupter circuit output with <20% duty cycle.

The external interrupter circuit was flashed successfully and was working as expected. Due to previous component failures, our hardware testing mostly comprised of checking working connections with a multimeter, being able to verify that the rest of the components were still working and were connected properly.

4. Cost

4.1. Parts

The total parts cost of the list mentioned in Appendix A (Table A.1.) comes out to \$216.16.

4.2. Labor

With each person putting in about 17-18 hours of work in a week - amounting to about 175 hours per person throughout the project - our team had the following distribution of hours across the project -

	Ali	Kartik
Circuit Design and debug	120	35
Microcontroller Setup, Interfacing and Debugging	45	125
Documentation and Writing	10	15

Setting the average wage to 35\$/hr over a 2.5-month period, we obtained our cost of labor as follows -

Wage	Total Labor Hours (monthly)	Labor Cost
35\$/hr	140	\$12,250

And given the cost of parts and labor, the total cost for our project comes out at **\$12,466.16**.

5. Conclusion

5.1. Accomplishments

Despite the Tesla coil itself not being able to arc, we learned a lot from the design process. For example, we had to learn FreeCAD for designing the tesla coil support and winding enclosure, along with STM32 documentation and HAL for programming and flashing our microcontroller.

The external interrupter was tested to be working as expected independent of the feedback controller subsystem, and the on-PCB MCU was flashed successfully.

We recognize that individual breadboard prototyping of more than just the PFC subsystem in order to test individual subsystems thoroughly - in addition to having demonstrable portions in the case of issues arising within a certain subsystem - is a valuable lesson learnt from this endeavor.

5.2. Uncertainties

Due to critical component failures we were unable to properly verify the working of our subsystems, and would be unable to pinpoint the cause of other issues that may have risen after replacing defective or broken parts.

5.3. Ethical considerations

We referenced the IEEE Recommended Practices for Safety in High-Voltage and High-Power Testing while building up and testing our subsystems.

The ACM [1] and IEEE Code of Ethics were important considerations during every step of our design, and combined with the recommended practices was a contributing factor to recognizing the danger of continuing testing.

In addition to working with high-voltage, the damaged optic receiver was a major setback as we lost the ability to control the coil from a safe distance away from sensitive electronics as per the FCC standards for Electromagnetic Interference (EMI). The Tesla Coil subsystem was to be tested last in order to ensure that our design worked as expected. However, the failure of a MOSFET in the gate drive subsystem due to an unintentional short made further testing unfeasible due to safety concerns.

5.4. Future work

Despite the nature of tesla coils being largely confined to being niche hobbyist projects and setbacks faced in this project, we are confident in the working of our design and believe that the power-efficiency achieved by this tesla coil design will significantly reduce the strain placed by similar future designs on power grids, allowing for more widespread access to tesla coils in rural areas.

6. References

[1] “ACM code of ethics and professional conduct,” Association for Computing Machinery, 2018. Available:

<https://www.acm.org/code-of-ethics>

[2] “How the Boost PFC Converter Circuit Improves Power Quality - Technical Articles”, www.allaboutcircuits.com. Available:

<https://www.allaboutcircuits.com/technical-articles/how-the-boost-pfc-converter-circuit-improves-power-quality/>

[3] “Universal DRSSTC Driver 2.7.”, G.Guangyan. Available: <https://loneoceans.com/labs/ud27/>

[4] “A Table-top Musical Tesla Coil, Double Resonant Solid State”, G.Guangyan. Available:

<https://loneoceans.com/labs/drsstc1/>

[5] Infineon Application Note, “PFC Boost Converter Design Guide,” S.Abdel-Rahman .F.Stuckler, K.Siu. Available:

https://www.infineon.com/dgdl/InfineonApplicationNote_PFCCMBoostConverterDesignGuide-AN-v0200-EN.pdf?fileId=5546d4624a56eed8014a62c75a923b05

[6] STMicroelectronics Application Note, “Digital PFC and dual FOC MC integration.” Available:

https://www.st.com/resource/en/application_note/cd00266366-digital-pfc-and-dual-foc-mc-integration-stmicroelectronics.pdf

[7] Onsemi, IGBT – “IGBT Field Stop 650 V, 60 A”, FGA60N65SMD,

<https://www.onsemi.com/download/data-sheet/pdf/fga60n65smd-d.pdf>

[8] STMicroelectronics, “650 V, 12 A power Schottky silicon carbide diode”, STPSC12065,

<https://www.mouser.com/datasheet/2/389/stpsc12065-1851867.pdf>

[9] STMicroelectronics, “Medium-density performance line Arm®-based 32-bit MCU with 64 or 128 KB Flash, USB, CAN, 7 timers, 2 ADCs, 9 com. Interfaces”, STM32F103,

<https://www.mouser.com/datasheet/2/389/stm32f103c8-1851025.pdf>

[10] STMicroelectronics Application, “Guidelines for oscillator design on STM8AF/AL/S and STM32 MCUs/MPUs”, pp.10-27. Available:

https://www.st.com/resource/en/application_note/an2867-guidelines-for-oscillator-design-on-stm8afals-and-stm32-mcusmpus-stmicroelectronics.pdf

[11] “Solid State Tesla Coils,” web page. Available at:

<https://stevehv.4hv.org/SSTCindex.htm>. Accessed May 2025.

[12] Biricha.Step-by-step Digital PFC Design using STM32. October 2020. Accessed May 2025.[Online Video]. Available: <https://www.youtube.com/watch?v=Gow8cdyuRIY>.

Appendix A: Parts List, Requirement and Verification Table

Part	Quantity	Part link	Cost
36 AWG copper wire	328ft	https://www.remingtonindustries.com/content/Polyurethane%20Magnet%20Wire%20Data%20Sheet.pdf	\$15.00
14 AWG copper wire	15.24m (4.572m used)	https://www.southwire.com/wire-cable/building-wire/thhn-thwn-copper-silicone-free/p/11579001	\$30.00
P-N combo for GDT drive	2	https://www.digikey.com/en/products/detail/vishay-siliconix/SQJ560EP-T1-GE3/9462337	\$4.06
560μF Bulk Capacitor for DC rail	1	https://www.digikey.com/en/products/detail/panasonic-electronic-components/EE-T-UQ2G561EA/483502	\$4.16
Film Decoupling Capacitor for DC rail	3	https://www.digikey.com/en/products/detail/wima/MKP4J041006D00KSSD/9370504	\$9.03
Ferrite cores for CTs and GDT	5	https://www.digikey.com/en/products/detail/epcos-tdk-electronics/B64290L0674X830/1830199	\$26.65
Schottky diodes	10	https://www.digikey.com/en/products/detail/stmicroelectronics/1N5819RL/1037327	\$1.69
GDT gate driver	1	https://www.digikey.com/en/products/detail/texas-instruments/UCC27423P/60326	\$1.21

		Q	
Fiber transmitter for interrupter	1	https://www.digikey.com/en/products/detail/industrial-fiber-optics/IF-E96E/3461614	\$6.66
Fiber receiver for interrupter	1	https://www.digikey.com/en/products/detail/industrial-fiber-optics/IF-D95T/243780	\$8.91
Plastic optic fiber for interrupter	5 meters	https://www.digikey.com/en/products/detail/industrial-fiber-optics/GH4001/22535727	\$8.34
IGBTs for power stage and PFC	3	https://www.digikey.com/en/products/detail/onsemi/FGA60N65SMD/3137189	\$19.62
SiC Schottky for PFC	1	https://www.digikey.com/en/products/detail/stmicroelectronics/STPSC12065DY/6051095	\$4.29
Flip Flops for Feedback Controller	2	https://www.mouser.com/ProductDetail/Texas-Instruments/SN74LS74ADR?qs=UG%2F8xqv%2F6WdOEnCo3YslYA%3D%3D	\$0.96
AND gate	3	https://www.digikey.com/en/products/detail/texas-instruments/sn74ls08n/277279	\$2.22
Gate driver for PFC switch	1	https://www.digikey.com/en/products/detail/microchip-technology/MCP1407-E-P/1228640	\$1.25
Current Sense Amplifier	1	https://www.digikey.com/en/products/detail/texas-instruments/INA281A2QDBVRQ1/13566882	\$2.61
Bridge Rectifier	1	https://www.mouser.com/ProductDetail/	\$1.53

		Taiwan-Semiconductor/GBU1506?qs=81r%252BiQLm7BTsXs%252BQWRWWIA%3D%3D	
Schmitt Trigger hex inverter	4	https://www.mouser.com/ProductDetail/Texas-Instruments/SN74LS14NE4?qs=sGA%3EpiMZZMutXGli8Ay4kP28D9wZ8SQIn6ZUb2xkzdw%3D	\$6.72
LM311 comparator for OCP	1	https://www.digikey.com/en/products/detail/texas-instruments/LM311P/277038	\$0.41
Differential comparator for feedback	1	https://www.mouser.com/ProductDetail/Texas-Instruments/TL3116IDR?qs=odmYg%3EirbwwN4qt6U49uyg%3D%3D	\$3.46
HSE crystal	1	https://www.digikey.com/en/products/detail/cts-frequency-controls/ATS080B-E/2292902	\$0.21
STM32F103C8 Microcontroller	1	https://www.digikey.com/en/products/detail/stmicroelectronics/STM32F103C8T6TR/2122442	\$6.08
PCB	5	9758330A_Y1_250411	\$60

Table A.1. Parts List with overall cost per part.

Subsystem Requirements	Verification requirements and method	Verification status
1. Feedback Controller 1.1. Electrical Isolation: The interrupter signal receiver must provide complete electrical isolation between	Feedback Controller No measurable conduction ($0\ \Omega$) between the interrupter device and the Tesla coil,	N

<p>the interrupter device and the Tesla coil.</p> <p>1.2. Total propagation delay: The feedback logic must be fast enough to ensure a zero-crossing detection propagates quickly enough to the power stage drivers for it to be effective.</p> <p>1.3. Zero-Crossing Detection: The feedback controller must accurately detect zero-crossing events to ensure smooth operation of the Tesla coil.</p>	<p>verified using a multimeter.</p> <p>Total propagation delay must be less than 2 μs to ensure proper synchronization with the Tesla coil's resonant frequency.</p> <p>Zero-crossing detection accuracy must be within $\pm 2 \mu$s.</p>	<p>N</p> <p>N</p>
<p>2. PFC Stage</p> <p>2.1. Output Voltage: The PFC stage must output a DC voltage between 350 V and 400 V for the power stage.</p> <p>2.2. Switching Frequency: The boost converter must operate at a switching frequency of roughly 100 kHz.</p> <p>2.3. The gate driver must provide sufficient drive signals to the IGBT in the boost converter.</p>	<p>PFC Stage</p> <p>No measurable conduction (0 Ω) between the interrupter device and the Tesla coil, verified using a multimeter.</p> <p>Total propagation delay must be less than 2 μs to ensure proper synchronization with the Tesla coil's resonant frequency.</p> <p>Zero-crossing detection accuracy must be within $\pm 2 \mu$s.</p>	<p>N</p> <p>N</p> <p>N</p>

<p>3. Tesla Coil</p> <p>Capacitor Protection: Capacitors should not be destroyed under normal operating conditions.</p> <p>Coupling Coefficient: The coupling coefficient between the primary and secondary windings must be kept low (< 0.3) to ensure a slow and safe ramp-up.</p> <p>Resonant Frequency: We should be able to adjust the resonant frequency of the primary without issue by adding or removing windings from the primary.</p>	<p>Tesla Coil</p> <p>No measurable conduction ($0\ \Omega$) between the interrupter device and the Tesla coil, verified using a multimeter.</p> <p>Total propagation delay must be less than $2\ \mu\text{s}$ to ensure proper synchronization with the Tesla coil's resonant frequency.</p> <p>Zero-crossing detection accuracy must be within $\pm 2\ \mu\text{s}$.</p>	<p>Y</p>
<p>4. Power Stage</p> <p>Voltage Handling: The IGBT half-bridge must withstand a minimum input voltage of 400 VDC (the expected maximum output of the PFC) with sufficient headroom.</p> <p>Switching Frequency: The IGBTs must operate at a minimum switching frequency of 300 kHz without excessive switching losses.</p> <p>Gate Drive: The gate drive transformer (GDT) must</p>	<p>Power Stage</p> <p>No measurable conduction ($0\ \Omega$) between the interrupter device and the Tesla coil, verified using a multimeter.</p> <p>Total propagation delay must be less than $2\ \mu\text{s}$ to ensure proper synchronization with the Tesla coil's resonant frequency.</p>	

provide sufficient drive signals to the IGBTs.	Zero-crossing detection accuracy must be within $\pm 2 \mu\text{s}$.	
--	---	--

Table A.2. Requirements and Verification Table.

Appendix B: JavaTC specification

OPTIONS

Select Units <input type="text" value="inches"/>	Ambient Temperature 68 <input type="text" value="Fahrenheit"/>	Secondary Wire Material Copper: <input checked="" type="checkbox"/> Aluminum: <input type="checkbox"/>	Primary Wire Material Copper: <input checked="" type="checkbox"/> Aluminum: <input type="checkbox"/>	Primary Wire Type Round: <input checked="" type="checkbox"/> Ribbon: <input type="checkbox"/>	Primary Capacitor (µF) 0.1	<button>Load Demo Coil</button>	<button>Load Saved Coil</button>
---	--	--	--	---	-------------------------------	---------------------------------	----------------------------------

FLOOR & SURROUNDINGS

Ground Radius <input type="text" value="0"/>	Wall Radius <input type="text" value="0"/>	Ceiling Height <input type="text" value="0"/>
---	---	--

SECONDARY COIL

Radius 1 (LV end) <input type="text" value="1.2"/>	Radius 2 (HV end) <input type="text" value="1.2"/>	Height 1 (LV end) <input type="text" value="5"/>	Height 2 (HV end) <input type="text" value="15"/>	Turns <input type="text" value="1700"/>	AWG: <input checked="" type="checkbox"/> Wire Dia: <input type="text" value="36"/>
---	---	---	--	--	--

PRIMARY COIL

Radius 1 (LV end) <input type="text" value="1.75"/>	Radius 2 (HV end) <input type="text" value="1.75"/>	Height 1 (LV end) <input type="text" value="5"/>	Height 2 (HV end) <input type="text" value="5.6"/>	Turns <input type="text" value="5.7"/>	AWG: <input checked="" type="checkbox"/> Wire Dia: <input type="text" value="14"/>
Ribbon Height <input type="text" value="0"/>	Ribbon Thickness <input type="text" value="0"/>	Total Lead Length <input type="text" value="0"/>	Lead Wire Diameter <input type="text" value="0"/>		

TOROID

Toroid Minor Diameter <input type="text" value="2"/>	Toroid Major Diameter <input type="text" value="8"/>	Toroid Center Height <input type="text" value="15"/>	Connection Topload: <input checked="" type="checkbox"/> Ground: <input type="checkbox"/>	Count: 1 <button>Add</button> <button>Remove</button> <button>Edit</button> #1: minor=2, major=8, height=15, topload #2: #3:
---	---	---	--	---

SPHERE

Sphere Horizontal Diameter <input type="text" value="0"/>	Sphere Vertical Diameter <input type="text" value="0"/>	Sphere Center Height <input type="text" value="0"/>	Connection Topload: <input checked="" type="checkbox"/> Ground: <input type="checkbox"/>	Count: 0 <button>Add</button> <button>Remove</button> <button>Edit</button> #1: #2: #3:
--	--	--	--	--

DISC

Disc Inside Diameter <input type="text" value="0"/>	Disc Outside Diameter <input type="text" value="0"/>	Disc Height <input type="text" value="0"/>	Connection Topload: <input checked="" type="checkbox"/> Ground: <input type="checkbox"/>	Count: 0 <button>Add</button> <button>Remove</button> <button>Edit</button> #1: #2: #3:
--	---	---	--	--

CYLINDER

Cylinder Diameter <input type="text" value="0"/>	Cylinder Bottom Height <input type="text" value="0"/>	Cylinder Top Height <input type="text" value="0"/>	Connection Topload: <input checked="" type="checkbox"/> Ground: <input type="checkbox"/>	Count: 0 <button>Add</button> <button>Remove</button> <button>Edit</button> #1: #2: #3:
---	--	---	--	--

Auto-Tune: ☐ Adjust Coupling: RUN JAVATC RESET

SECONDARY COIL OUTPUT DATA			PRIMARY COIL OUTPUT DATA		
Secondary Resonant Frequency	271.34	kHz	Primary Resonant Frequency	229.43	kHz
Angle of Secondary	90	deg °	Percent Detuned	15.45	% high
Length of Winding	10	inch	Angle of Primary	90	deg °
Turns Per Unit	170	inch	Length of Wire	5.22	ft
Space Between Turns (e/e)	0.00088	inch	DC Resistance	13.19	mOhms
Length of Wire	1068.1	ft	Space Between Turns (e/e)	0.041	inch
H/D Aspect Ratio	4.17	:1	Proximity	0.515	inch
DC Resistance	439.4948	Ohms	Recommended Minimum Proximity	0	inch
Reactance at Resonance	66048	Ohms	Primary Inductance-Ldc	4.812	µH
Weight of Wire	0.08	lbs	Resonant Tank Cap Reference	0.07149	µF
Effective Series Inductance-LES	38.739	mH	Primary Lead Inductance	0	µH
Equivalent Energy Inductance-Lee	39.568	mH	Mutual Inductance	82.945	µH
Low Frequency Inductance-Ldc	37.92	mH	Coupling Coefficient	0.194	k
Effective Shunt Capacitance-Ces	8.881	pF	Recommended Coupling Coefficient	0.124	k
Equivalent Energy Capacitance-Cee	8.695	pF	Energy Transfer	5.15	1/2 cycle
Low Frequency Capacitance-Cdc	15.476	pF	Total Energy Transfer Time	10.97	µs
Topload Effective Capacitance	7.162	pF			
Skin Depth	5.75	mils			
AC Resistance	545.4636	Ohms			
Secondary Q	121				

Appendix C: Pinout and Code Documentation

```
/* Private user code -----*/
/* USER CODE BEGIN 0 */

volatile uint16_t adcResults[2][2]; //DMA buffers [0][0]=output voltage, [1][0]=input current, [1][1]=input voltage
volatile uint8_t currentBuffer = 0;

void HAL_TIM_PeriodElapsedCallback(TIM_HandleTypeDef *htim)
{
    if (htim == &htim3)
    {
        //falling edge of 80kHz timer
        if (currentBuffer == 0)
        {
            //start output voltage measurement
            HAL_ADC_Start_DMA(&hadc1, (uint32_t*)&adcResults[0][0], 1);
            currentBuffer = 1;
        }
        else
        {
            //start input current and voltage measurements
            HAL_ADC_Start_DMA(&hadc1, (uint32_t*)&adcResults[1][0], 1); //input current
            HAL_ADC_Start(&hadc2); //input voltage
            currentBuffer = 0;
        }
    }
}

void HAL_ADC_ConvCpltCallback(ADC_HandleTypeDef* hadc)
{
    if (hadc == &hadc2)
    {
        //input voltage conversion complete
        adcResults[1][1] = HAL_ADC_GetValue(&hadc2);

        //all three measurements are ready - run control algorithm
        RunControlAlgorithm(adcResults[0][0], adcResults[1][0], adcResults[1][1]);
    }
}
```

Private Functions for callback.

```

void RunControlAlgorithm(uint16_t outputVoltage, uint16_t inputCurrent, uint16_t inputVoltage)
{
    //convert ADC readings to real values
    float v_out = outputVoltage_adc * V_CORRECTION_FACTOR;
    float v_in = inputVoltage_adc * V_CORRECTION_FACTOR;
    float i_in = inputCurrent_adc * IIN_CORRECTION_FACTOR;
    float v_rms = 0.707 * v_in;

    static float target_v_out = 400.0f; //our target output voltage

    //calculate demand current for PFC
    float i_demand = (v_in)*(v_out) / (v_rms)^2;

    //current error for PFC control
    float current_error = i_demand - i_in;

    // PI controller for PFC
    pfc_integral += current_error;

    //anti-windup
    if (pfc_integral > 0.5f/KI_PFC) pfc_integral = 0.5f/KI_PFC;
    if (pfc_integral < -0.5f/KI_PFC) pfc_integral = -0.5f/KI_PFC;

    //duty cycle calculation
    float duty = KP_PFC * current_error + KI_PFC * pfc_integral;

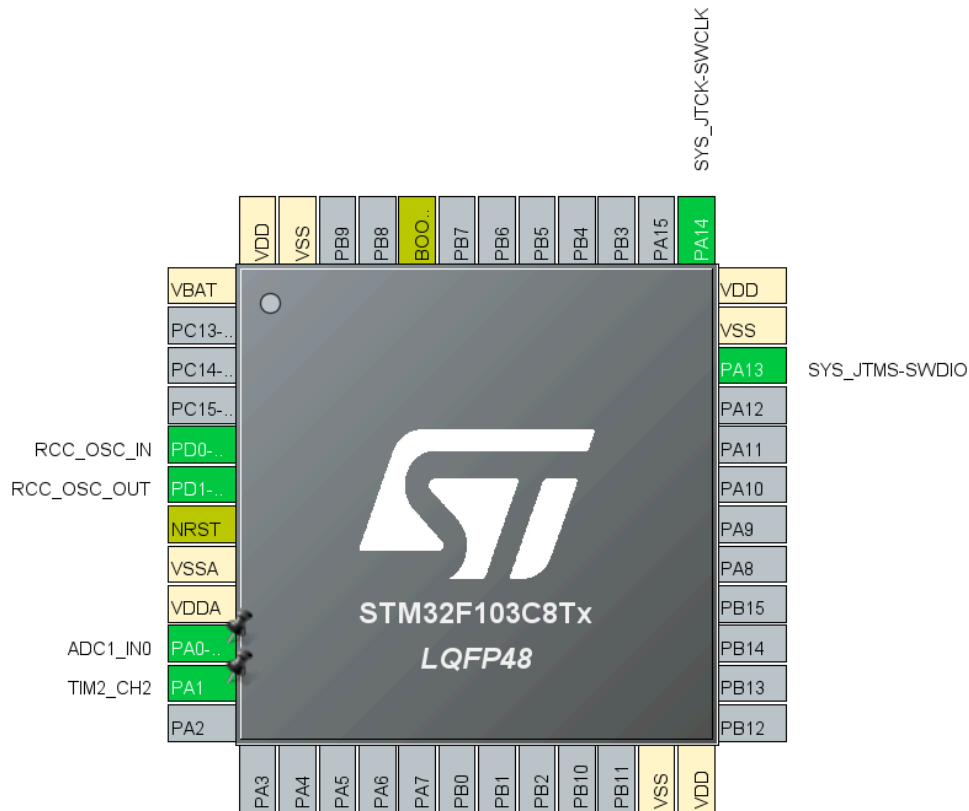
    //feed-forward term based on input/output voltage ratio
    float feed_forward = 1.0f - (v_in / target_v_out);
    duty += feed_forward;

    //clamp duty cycle
    if (duty > MAX_DUTY) duty = MAX_DUTY;
    if (duty < MIN_DUTY) duty = MIN_DUTY;

    //update PWM
    uint32_t pwmValue = (uint32_t)(duty * htim3.Init.Period);
    __HAL_TIM_SET_COMPARE(&htim3, TIM_CHANNEL_4, pwmValue);
    //timer's duty cycle is half of PWM
    __HAL_TIM_SET_COMPARE(&htim3, TIM_CHANNEL_3, pwmValue/2);
}
/* USER CODE END 0 */

```

Control Algorithm.



Interrupter circuit STM pinout

```

/* Infinite loop */
/* USER CODE BEGIN WHILE */
while (1)
{
    //HAL_GPIO_TogglePin(DummySignal_GPIO_Port, DummySignal_Pin); //simple Blink fn. Use for testing.
    //HAL_Delay(50);

    //void MonitorADCLoop();
    HAL_ADC_PollForConversion(&hadc1, 10);
    adc_value = HAL_ADC_GetValue(&hadc1);
    uint32_t pwm_compare = (adc_value*20 / 4095); //0-80% range

    //clamp to avoid 0% or 100% (safety)
    if (pwm_compare > 30) pwm_compare = 20;
    //if (pwm_compare < 10) pwm_compare = 10;

    // Update PWM duty cycle
    __HAL_TIM_SET_COMPARE(&htim2, TIM_CHANNEL_1, pwm_compare);
}
/* USER CODE END WHILE */

/* USER CODE BEGIN 3 */
}

```

Interrupter circuit code to adjust PWM based on potentiometer.